Urban Heat Island Effect in the Rotterdam Harbour and Its Relationship with Surface Materials and Site Design

Erasmus University College

Wouter van Wijngaarden

EUC Capstone - CAP400

Major: *Life Sciences*

Supervisor: *Dr. Sergio Mugnai*

Word Count: 6069

Date: 06/06/2025

Keywords: Urban Heat Island (UHI), Thermal Performance, Industrial Port Areas, Microclimate Mapping, Rotterdam Harbour, Surface Material.

Acknowledgements

I would like to thank the following people for helping with this research project:

Representatives of Erasmus University College, the Rotterdam Heat Lab, Delft Green Village and TU Delft for their willingness to impart their knowledge.

All the harbour security officers and Maple Group team members who took the time to show me around the terminal, and my dad, who contributed through his further comments and helpfulness. Sophia for her patience and encouragement. I would particularly like to thank the experts from TU Delft who agreed to be my research partner and secondary grader, Daniela and Max. Kinshuk for his help with statistics, and my dear friend Robin, because I keep my promises.

List of Abbreviations

Term	Definition
UHI	Urban Heat Island
IHI	Industrial Heat Island
SHI	Surface Heat Island
WBGT	Wet Bulb Globe Temperature
QGIS	Quantum Geographic Information System
GIS	Geographic Information System
T	(Kestrel 5400 Heat Stress) Tracker
MODIS	Moderate Resolution Imaging Spectroradiometer (satellite sensor)

Table of Contents

Abstract

The urban heat island effect, characterised by high temperatures in urban areas compared to their rural surroundings, is especially noticeable in industrial port environments due to their unique environment and material characteristics. This thesis investigates the thermal dynamics of the Rotterdam Harbour, Europe's largest industrial port, focusing on the relationship between surface materials, site design, and local microclimate variation. The motivation for this study is the growing vulnerability of industrial areas to heat stress under the threat of climate change because of their unique dense infrastructure, sparse vegetation, and large impervious surfaces. These factors contribute to local warming and present significant challenges to worker safety and climate adaptation in Rotterdam. The central research question is "*What morphological factors contribute to the variation in thermal performance of the Rotterdam Harbour?".* Employing a mixed-methods approach, the study integrates empirical field measurements at a pilot site in Pernis with spatial analysis using geographic information systems and a review of relevant literature. The methodology includes surface temperature mapping, identifying material thermal characteristics, and microclimate observations, allowing for a nuanced assessment of how different industrial environmental factors impact thermal conditions. The main findings reveal that areas dominated by asphalt, concrete, and metal exhibit the highest surface temperatures, while compact and enclosed building arrangements further exacerbate heat retention. Conversely, adaptations in green infrastructure, surface colour and strategic spacing between buildings can lower local temperatures by several degrees, highlighting the potential for targeted interventions. The findings highlight the importance of climate-adaptive design strategies in industrial port planning, with a focus on material choice, spatial arrangement, and the use of vegetation to reduce localised heat. Ultimately, this research provides data-driven solutions for enhancing the thermal resilience of industrial port environments and informs policy recommendations improving urban sustainability in the face of a global heat crisis.

1. Introduction

1.1 Background

The urban heat island (UHI) effect describes the phenomenon where urban areas experience higher temperatures than their rural surroundings. This temperature difference is mainly driven by morphological factors, meaning the physical characteristics and spatial arrangement of the local environment. Morphological factors include the types of materials used in the constructions, the density and placement of buildings and infrastructure, and the extent of vegetation present within an area (Deilami et al., 2018). Increased building density, reduced green space, and the use of heat-retentive materials such as concrete and asphalt all contribute to greater heat absorption and retention in cities. These attributes shape how urban environments interact with solar radiation, store its heat, and ultimately influence local microclimates. Because individuals living in cities are more susceptible to localised heat stress, the impacts of UHIs have significantly increased due to accelerated climate change. This concentrated heat also increases risks of serious health problems for the general population, the need for energy for cooling, and makes cities less liveable, particularly during heat waves (Norton et al., 2015; RIVM, 2021).

Because industrial zones are extensively made up of impermeable surfaces such as concrete, asphalt, and metal, they are especially vulnerable to the impacts of UHIs. (Voogt & Oke, 2003). The biggest industrial location in Europe, the Rotterdam Harbour and its increased susceptibility to heat stress have resulted in a recent increase in research on the distinctive design of industrial areas (Klok et al., 2012). Recent studies have indicated the rise of 'industrial heat islands' (IHIs), in which groups of industrial operations produce localised warming that is different from the overall urban environment (Meng et al., 2021; Yüksel & Yılmaz, 2008). Industrial regions like the Rotterdam Harbour tend to experience the most

pronounced warming during the summer months, coinciding with periods of greatest heat risk (Meng et al., 2021).

These elements highlight how important it is to conduct focused heat risk assessments and create customised mitigation plans to improve urban sustainability and thermal resilience in industrial port settings.

1.2 Research context

This study was carried out in connection with the Rotterdam Heat Lab, a Resilient Delta program initiative to address the growing issue of heat stress in the Rotterdam region. This program gives students the chance to actively participate in creative solutions for urban heat within the Rotterdam Heat Lab, through working with local stakeholders and experts to address pressing issues of heat in the city. This research paper is an illustration of this cooperative approach where professionals, researchers, and students collaborate to create a city that is healthier, more resilient, and cooler.

1.3 Research Problem and Objectives

Although industrial areas within the Rotterdam Harbour have been identified as thermal hotspots, few studies have explored the precise morphological factors that contribute to thermal performance in industrial zones, especially in the context of port settings (Xiao et al., 2018). Therefore, this thesis aims to tackle this problem through a case study of the Port of Rotterdam, by using a pilot site in Pernis, to explore how spatial patterns in industrial settings impact local microclimates. The first-hand field analysis was carried out at the Maple Group terminal in Pernis. Assistant Professor Dr. Daniela Maiullari and Junior Researcher Max van der Waal from Delft University of Technology assisted in selecting and visiting the site. Through the integration of geographical and empirical data, the study seeks to evaluate how well existing landscape layouts mitigate solar heat exposure.

1.4 Structure of the Thesis

The main research question that guides this thesis is: *What morphological factors contribute to the variation in thermal performance of the Rotterdam Harbour?*

The structure of the thesis is as follows: The theoretical background and relevant literature on urban and industrial heat islands are reviewed in Chapter 2. The methodology, including site selection, data collection, and analytical tools, is covered in detail in Chapter 3. The Pernis pilot site's spatial and visual analysis is presented in Chapter 4, supplemented by aerial imagery (Figure 4) and QGIS mapping (Figure 8). Chapter 5 analyses the field data measurements, interpreting the relationships between morphological factors and observed thermal variations. Finally, the consequences for climate adaptation and recommendations for improving the infrastructure of Rotterdam's port will be discussed.

2. Literature Review

2.1 Urban Heat Islands in Industrial Zones

Luke Howard (1833) was the first to document the phenomenon of heat islands in the early 19th century when he observed that London was warmer than it usually was than the nearby countryside. Urbanisation, which modifies surface materials, spatial arrangements, and the addition of new heat sources, is the cause of this effect. The way heat is absorbed, stored, and released has been drastically transformed as cities grow denser and replace natural landscapes with urban spaces (Oke, 1982; Norton et al., 2015). Oke (1982) laid the groundwork for later urban climate modelling by offering a methodical scientific framework for comprehending the energy exchanges that lead to the formation of UHI (Voogt & Oke, 2003). As a result of their poor solar reflectivity (albedo) and high thermal capacity (how much heat energy a substance can absorb), these materials collect more solar energy during the day and release it gradually at night, which persistently keeps cities warm (Mohajerani et al., 2017; Stewart & Oke, 2012).

A growing body of research is now distinguishing between the traditional UHI and the Industrial Heat Island (IHI) effect (Meng et al., 2021). In contrast to residential areas, which frequently take advantage of the natural cooling effects of evaporation from green spaces and tree cover, industrial zones are characterised by a lack of vegetation and vast stretches of impermeable surfaces (Xiao et al., 2018; Shishegar, 2014). Heat accumulation is increased, and nighttime cooling is decreased due to the spatial organisation of factories, warehouses, and container yards as well as the prevalence of heat-retentive materials (Norton et al., 2015). Additionally, operational and fixed features of the port environment such as continuous machinery usage, process waste heat, and the concentration of big, flat-roofed structures, contribute to industrial heat islands in addition to their material characteristics (Yüksel & Yılmaz, 2008).

Figure 1 makes this spatial pattern quite evident. The image shows that industrial areas continuously have greater UHI values than their surrounding vegetation or water, emphasising the significant heat load in these areas (Klok et al., 2012; Gartland, 2008).

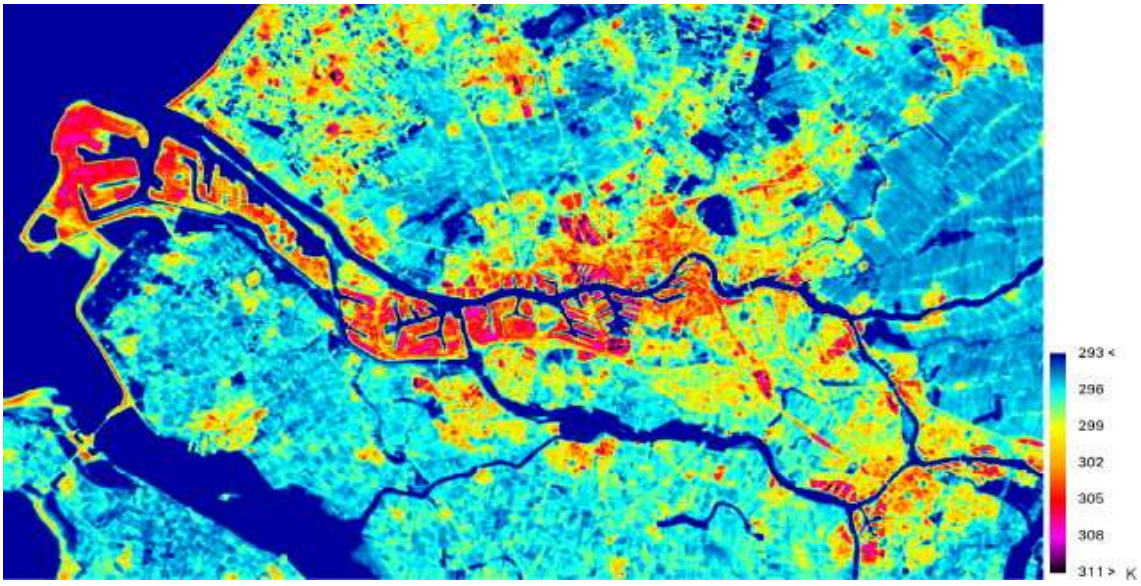

Figure 1
Surface heat island (SHI) intensity map of Rotterdam, derived from MODIS satellite data. Cooler tones signify lower temperatures in green spaces and water bodies, while warmer tones indicate higher surface temperatures

in industrial and urban regions. Adapted from "The surface heat island of Rotterdam and its relationship with urban surface characteristics," by Klok et al. https://doi.org/10.1016/j.resconrec.2012.01.009

2.2 Morphological Factors Influencing Thermal Performance

The morphological factors of industrial port regions mentioned earlier significantly influence their thermal environment. These factors interact to create unique UHI dynamics in industrial zones, setting them apart from residential areas and making them a critical focus for understanding local heat stress in the Rotterdam Harbour.

For instance, asphalt absorbs a significant amount of solar energy (albedo 0.05–0.20), which causes surface temperatures to rise by 15–20°C, relative to its surroundings, during periods of intense sunshine (Harmay & Choi, 2023; Roesler et al., 2016). Metal surfaces, which are common on industrial rooftops and container yards, heat up quickly and transmit this heat to the surrounding air due to their high conductivity, thus creating powerful local hotspots. Concrete, while somewhat more reflective, possesses significant thermal inertia, causing it to store heat throughout the day and release it slowly at night, thereby delaying cooling (Gartland, 2008; Mohajerani et al., 2017). When combined, these materials increase the area's ability to absorb and hold heat, which exacerbates the UHI impact in comparison to permeable or vegetated surfaces (Klok et al., 2012).

Thermal performance is also influenced by the way industrial zones are arranged spatially. Narrow service roads and large, low-rise buildings are characteristics of high-density layouts that limit natural ventilation and lower the possibility of convective cooling from the wind (Yuan & Chen, 2011; Van Hove et al., 2014). According to Stewart and Oke (2012), large warehouses and closely placed infrastructure reduce sky view factors and produce wind shadows, which trap heat at ground level and prevent radiative heat dissipation. Nonetheless, research shows that carefully placing buildings apart can improve ventilation and reduce local temperatures by 2–4°C (Chen et al., 2019). Therefore, depending on how

they promote or hinder air circulation, the placement of buildings and machinery in industrial settings can either increase or decrease thermal stress (Wang et al., 2024).

Recent studies have highlighted the possibilities of creative cooling techniques, such as applying reflecting coatings to pavements and roofs or using permeable paving materials that promote evaporative cooling (Mohajerani et al., 2017). These studies have shown a decrease in surface temperature, demonstrating the potential paths for future adaptation in Rotterdam Harbour, even if these technologies are not yet widely used in European ports.

One of the main natural deterrents to these heat-retentive characteristics is vegetation and green infrastructure, as they provide shade that lowers surface heat absorption and increases evaporative cooling by taking heat out of the atmosphere (Bowler et al., 2010; Norton et al., 2015). Studies have shown that even small additions of green infrastructure, like pathways lined with trees, can significantly lower surface temperatures in adjacent asphalt areas, frequently by several degrees Celsius (Xiao et al., 2018; Koc et al., 2018). Species selection (for example, broadleaf trees with large leaf area indices perform better than conifers) and spatial distribution determine how effective vegetation is in cooling (Shashua-Bar et al., 2011). Clustered plantings provide more microclimate advantages than isolated examples (Lopes et al., 2025). A viable method for reducing the urban heat island effect in industrial environments, in addition to vegetation, is the use of "cool pavement" technologies (Kappou et al., 2022). Generally, two factors can be altered to increase a pavement's reflectiveness: the pavement's colour and surface roughness (Mohajerani et al., 2017). Making pavement surfaces whiter, or as light-colored as feasible, is a practicable way to reduce the UHI effect, according to studies. A lighter pavement surface increases the quantity of light and heat radiation reflected into the atmosphere while decreasing the amount of solar radiation absorbed (Mohajerani et al., 2017).

As highlighted above, the distinct morphological makeup of industrial port areas is complicated and site-specific. To examine how these morphological features influence temperature variance in Rotterdam Harbour, this study applies a mixed-methods approach, drawing results from various data sources, detailed in the following section.

3. Methodology

3.1 Research Approach

This study integrates empirical field measurements, GIS-based spatial modeling, and qualitative literature analysis to investigate the morphological drivers of temperature variation in Rotterdam Harbour. This integration of quantitative and qualitative insights allows for a deeper understanding of how physical morphology shapes the thermal environment of the port (Clark, 2016). Combining these methods allows this research to utilise macro-scale spatial analysis, through QGIS, with micro-scale environmental data through field research. The three primary pillars supporting the research, therefore are:

1. **Literature Review**: The research paper was framed within the body of knowledge available about industrial thermal dynamics, UHIs, and the impact of material and morphological factors on microclimate by examining peer-reviewed literature. Emphasising material characteristics, the lack of vegetation, and the design of industrial zones, the review guided the analysis and interpretation of important variables for field and spatial analysis (Deilami et al., 2018; Norton et al., 2015). Among the key elements selected for spatial modelling based on this first study were the distribution of green space and building density.

2. **GIS-Based Spatial Analysis**: Spatial analysis was performed using Quantum Geographic Information Systems (QGIS) version 3.40.4. The Basisregistratie Grootschalige

Topografie (BGT), the Dutch national large-scale topography database, and the Publieke Dienstverlening Op de Kaart (PDOK), an open-access Dutch government geospatial data portal, provided high-resolution land use and material data. These databases offered comprehensive data on the distribution of green spaces in the study area, surface materials, and building footprints.

3. **Empirical Field Measurements*:*** On March 31, 2025, field measurements were taken at the Pernis pilot site. Kestrel 5400 Heat Stress Trackers were used to collect microclimatic data at three different zones, each of which represented a typical industrial microenvironment:

1. **Water's Edge Asphalt:** A paved, open space next to the waterfront that is close to the Eemhaven basin and receives direct sunlight.
2. **Open Container Landscape:** As a typical port logistics zone, this exposed area is dominated by stacked shipping containers and paved surfaces.
3. **Confined Empty Steel Container:** The inside of an empty steel shipping container, simulating an extreme enclosed industrial environment.

Microsoft Excel was used for data analysis, and each variable was analysed using the average (AVERAGE) and standard deviation (STDDEV.P) functions to quantify variability both within and between the microenvironments and to highlight central tendencies. Furthermore, temporal trends and spatial disparities were visualised using Excel's graphing capabilities, which ensured that every plot had an equal time axis for a simple comparison. Figure 2 provides a map of the greater Rotterdam Harbour area and highlights the location of the field study pilot site.

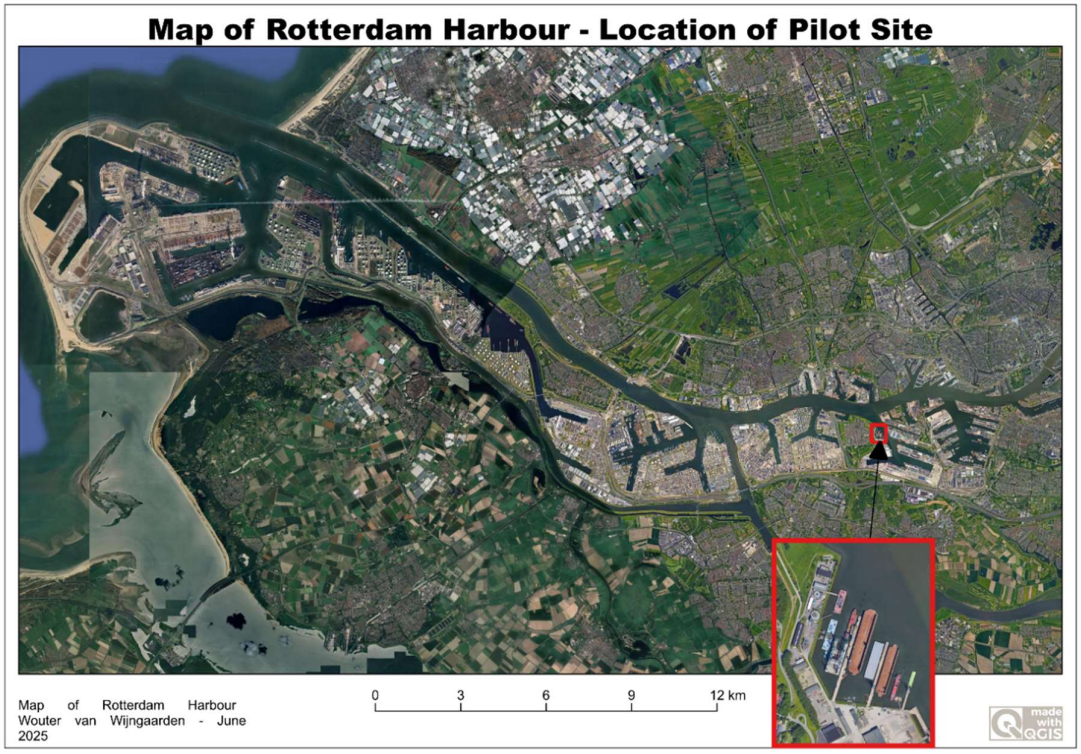

Figure 2

Map of the Rotterdam Harbour with the Location of the Pilot Site. ***The red box*** *(inset map) shows a zoomed-in view of the pilot site at the Maple Group terminal in Pernis.* ***The red marker with black arrow*** *indicates the exact location where environmental measurements were collected on March 31, 2025.* ***The scale bar*** *(0–12 km) is located at the bottom center of the map. North is oriented upward.* ***Coordinate system****: WGS 84 (EPSG:4326). Map created using QGIS.*

3.2 Literature Review

Peer-reviewed studies on industrial UHIs were retrieved, screened, and selected through a PRISMA 2020 systematic process (Page et al., 2021). This ensured alignment with the thesis's focus on morphological drivers of thermal variation in Rotterdam Harbour. The procedure followed stringent inclusion/exclusion guidelines and combined results with field measurements and QGIS spatial analysis to fill in research gaps on port-specific UHI. This review's inclusion and exclusion criteria guarantee a focused study of the structural factors that contribute to industrial UHIs in the contemporary Port settings, for the following reasons. Recent developments in measurement methods, methodology, and industrial climate adaptation have been included using only primary research studies that were published between 2010 and 2025. According to Klok et al. (2012) and Mohajerani et al. (2017), studies that met the eligibility requirements had to present empirical data on UHIs in industrial settings, specifically addressing important morphological factors like surface albedo, urban layout, or building materials. To guarantee accessibility and contextual relevance, only English-language or significant translated studies that were related to Rotterdam were taken into consideration. Non-peer-reviewed reports, opinion pieces, and review articles were excluded to preserve reliability and centre on empirical data. To account for the fundamental differences in thermal dynamics, research that exclusively concentrated on non-industrial settings was also disregarded (Yuan & Chen, 2011; Meng et al., 2021). The analysis of morphological effects on thermal performance in Rotterdam Harbour is directly supported by the literature thanks to this focused approach.

Table 1*. Reasons for Inclusion/Exclusion Based on Full-Text Screening*

Criterion	**Inclusion**	**Exclusion**
Publication Type	Primary research articles	Opinion pieces, review papers, non-peer-reviewed reports

Publication Date	2010–2025	Published before 2010
Language	English or significant English translation; Rotterdam-relevant works	Non-English publications without significant translation
Research Focus	Empirical data on UHIs in industrial settings	Studies focusing on residential or commercial UHIs only
Geographical Relevance	Studies relevant to Rotterdam or similar contemporary port/industrial areas	Studies on outdated or non-comparable urban morphologies
Variables Studied	Analysis of morphological factors (e.g., surface albedo, urban layout, materials)	Studies lacking empirical investigation of morphological factors
Technological Relevance	Use of modern measurement techniques and climate adaptation methods	Studies not reflecting recent developments in measuring technology or adaptation strategies

To align with the thesis's focus on morphological drivers of thermal variation in Rotterdam Harbour, the literature review identified, screened, and selected peer-reviewed studies on industrial UHIs using a systematic process that complied with PRISMA 2020 (Page et al., 2021). Strict inclusion/exclusion criteria were followed, and results were combined with field measurements and QGIS spatial analysis to fill in the gaps in port-specific UHI research. The screening of 114 uploaded sources is summarised in the figure below (see Figure 3 for structure):

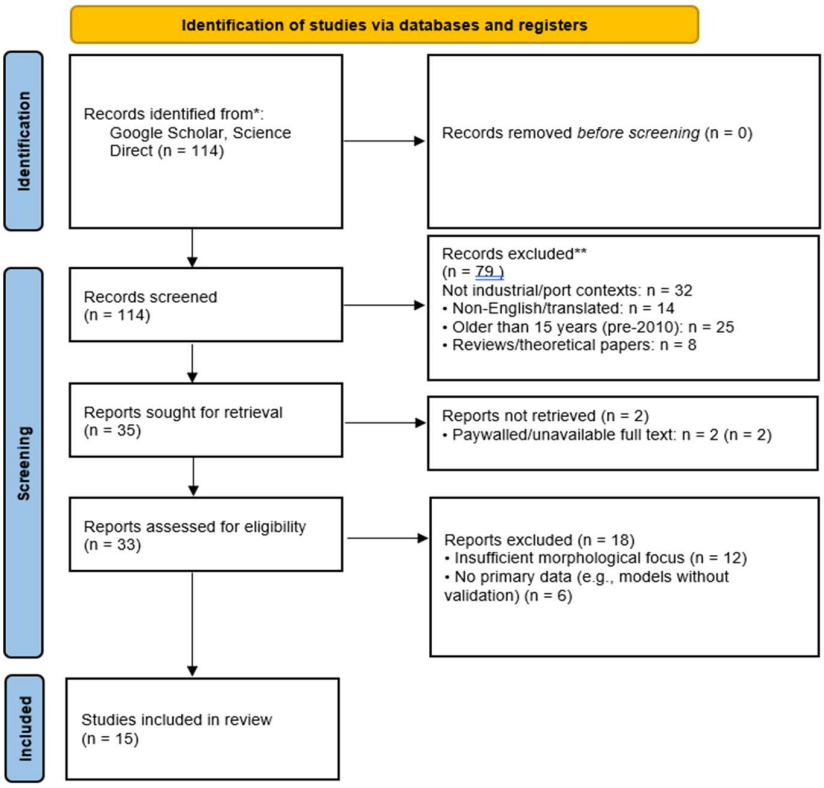

Figure 3. *PRISMA 2020 flow diagram illustrating the identification, screening, eligibility, and inclusion process for studies in this systematic review. Adapted from PRISMA 2020 flow diagram for new systematic reviews which included searches of databases and registers only (https://www.prisma-statement.org/PRISMAStatement/FlowDiagram).*

3.3 QGIS Spatial Analysis

In addition to its versatility, strong analytical capabilities, and compatibility with a variety of geospatial data types, Quantum Geographic Information Systems (QGIS) version 3.40.4 is a platform that is free to use and frequently used in urban research. QGIS makes it possible to spatially visualise, make maps and quantitatively evaluate the spatial correlations between urban form and heat patterns for the spatial analysis component of this work. High-resolution land use and surface material data were obtained from two key Dutch geospatial resources:

1. **Basisregistratie Grootschalige Topografie (BGT)**: The national large-scale topographical database of the Netherlands, which offers a wide range of current information on land cover, surface types, and building footprints.
2. **Publieke Dienstverlening Op de Kaart (PDOK)**: An open-access Dutch governmental portal offering downloadable geospatial datasets, including the BGT, for integration into GIS applications.

To map the spatial distribution of building density, green infrastructure, and materials throughout the Pernis pilot site, these datasets were imported into QGIS with the BGT Import dowloadable plugin. The material composition of container yards and roads, as well as building footprints, were extracted from BGT datasets and current satellite images using the PDOK material mapping database. For researchers wishing to replicate or extend this analysis, download links for QGIS and the PDOK BGT downloader are provided under Appendix D.

There are various benefits of using QGIS, because it is free and has a sizable user base, it is accessible for both academic and professional users. Its comprehensive spatial analysis tools make it feasible to integrate different data layers and provide analysis of the materials and urban layout. Since all processes and data sources can be shared and documented online, the platform encourages reproducibility. User created plug-ins like this made it possible to pinpoint the locations of regions that are mostly made of heat-retentive materials as well as their spatial relationships to nearby green spaces and bodies of water. The generated visualisations serve as the basis for the correlation between morphological traits and observed microclimatic parameters.

3.4 Field Observations in the Maple Group Site Pernis

An overhead perspective on the pilot site is shown in Figure 4, where the locations of the heat trackers are identifiable in the surrounding material environment and land cover. The image's numbers 1 through 3 represent the exact places where Kestrel 5400 WBGT Heat Stress Tracker (T) & Weather Meters were set up during the field activity, across the 200 by 70-meter Maple Group location. The measurements at the locations were started sequentially during the field campaign rather than all at once. Especially, the T3 measurement began later than T1 and T2 because of the order in which the temperature trackers were set up. Consequently, the total overlapping duration for all three trackers is fifteen minutes. This overlap, while brief, is sufficient for comparative analysis and ensures that the observed differences are not artifacts of changing external conditions. These three tracker sites were chosen under guidance from Dr. Daniela Maiullari to represent the variety of surface materials, spatial arrangements, and microclimatic factors that exist at the terminal, to collect data that is representative of the harbour environment. Data was collected on March 31, 2025, during a time of normal early spring weather in Rotterdam. Average outdoor temperatures on this day were around 8.2°C (4.4°C at the lowest and 12.0°C at the highest), with slightly cloudy skies.

Figure 4
Red numbers (1, 2, 3): Locations of environmental sensors, 1: ***T1*** *(Waterfront, adjacent to water and mixed surfaces), 2:* ***T2*** *(Terminal, in hardscaped industrial area), 3:* ***T3*** *(Container, inside a shipping container), Green areas: Urban greenery and parkland, Industrial zones: Hardscaped and containerized areas, Water: Eemhaven, a branch of the Nieuwe Maas. Retrieved May 7, 2025, from https://earth.google.com*

With its location on the bank of the river Nieuwe Maas and improved air flow, T1 is situated near the waterfront, next to the concrete and open water, where it could have a cooling effect compared to the interior locations of the Maple Group terminal. To measure this difference, T2 was situated in an open terrain area that is encircled by a large warehouse, containers, and industrial machinery like forklifts and cranes. This region is characteristic of the microclimate for port operations since it is large, paved, has no vegetation, and is exposed to direct sunlight. Inside a shipping container, T3 records thermal conditions in a confined, metal-dominated space that is notorious for its poor ventilation and excessive heat retention.

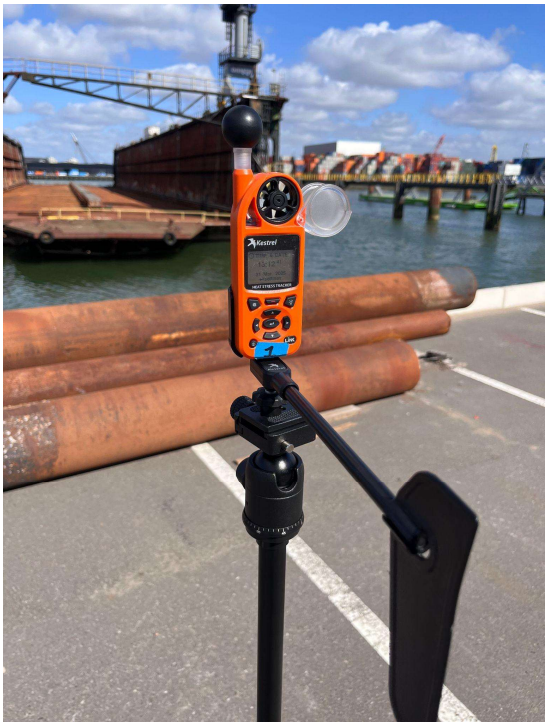

Figure 5
Ground-level view of the Kestrel 5400 Heat Stress Tracker at Site 1 (Waterfront), set up on asphalt adjacent to the Eemhaven waterfront (51° 53′ 14.22″ N, 4° 24′ 1.05″ E).

Figure 6
Ground-level view of the Kestrel 5400 Heat Stress Tracker 2 (Terminal), positioned on paved terrain surrounded by industrial containers and equipment (51° 53′ 15.58″ N, 4° 23′ 50.67″ E).

Figure 7
Interior of the steel shipping container at Site 3 (Container), showing the measurement environment for the third sensor (51° 53′ 15.55″ N, 4° 23′ 52.31″ E).

4 Results

4.1 QGIS Spatial Analysis

The clear morphological and land cover contrasts between the industrial port zone and the nearby residential neighbourhood are visualised by the QGIS spatial analysis of the Maple Group terminal area in Pernis. The map, as shown in Figure 8, combines field observations and BGT data. Surface types are colour-coded to signify their geographical distribution and their influence on the local microclimate.

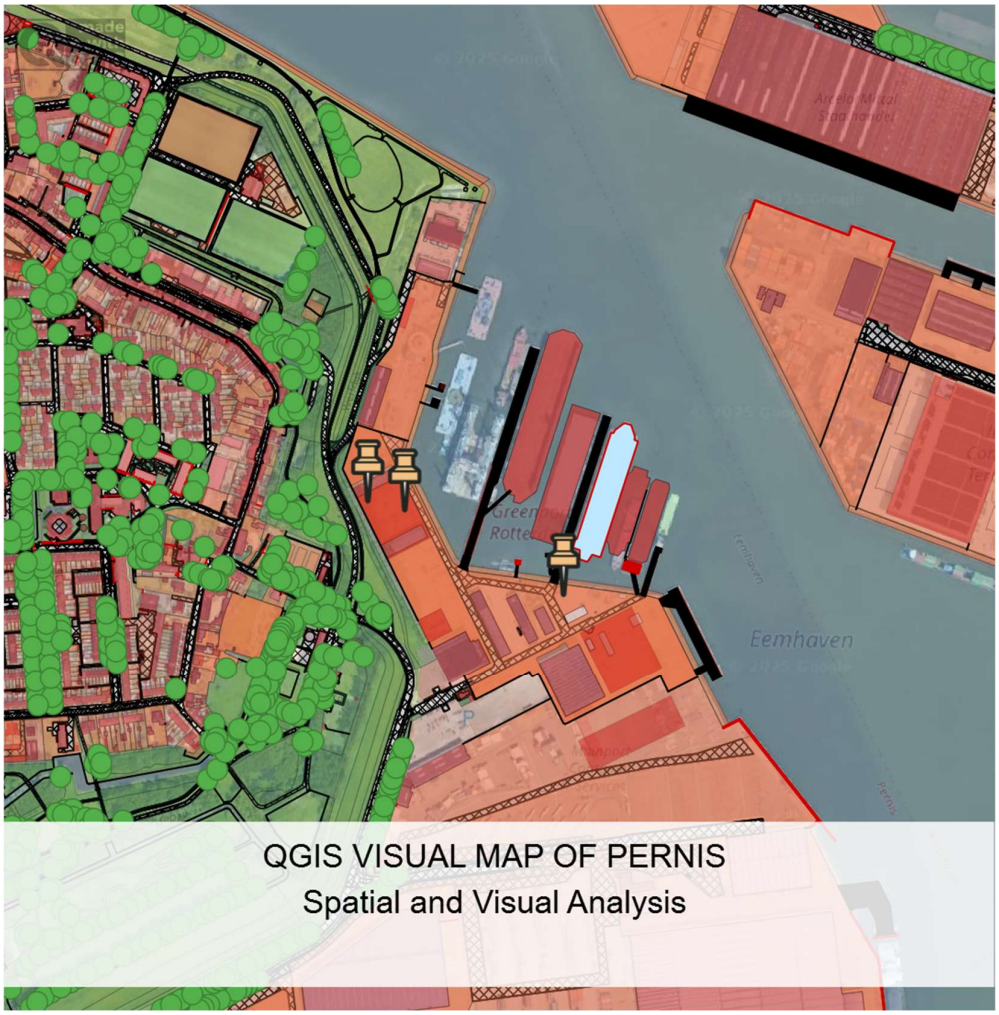

Figure 8
Spatial distribution of surface cover types at the Maple Group pilot site in Pernis, Rotterdam Harbour, visualised using QGIS (51° 53' 14.34" N, 4° 23' 57.62" E). ***Green****: Vegetation (trees, bushes, parks),* ***Red****: Impermeable surfaces (asphalt, cement, container yards),* ***Dark Red****: Warehouses and industrial buildings,* ***Black****: Roads,* ***Blue****: Water bodies (harbour, docks),* ***Pins*** *T1, T2, T3: Field measurement stations*

The most noticeable aspect of the spatial arrangement is the clear separation, created by a continuous green corridor, between the industrial terminal (to the east/right) and the Pernis residential neighbourhood (to the west/left). The highly populated residential buildings and the impermeable, heat-retentive port surfaces are separated by this green corridor, which is marked in green and is made up of parks, tree lines, and vegetated embankments. The residential neighbourhood itself is distinguished by a large percentage of green-coloured vegetated surfaces, such as street trees, tiny parks, and private gardens. By providing shade

and allowing for evapotranspiration, these vegetated zones are known to improve local cooling and occupants' thermal comfort (Bowler et al., 2010).

On the other hand, impermeable surfaces, shown in red, dominate the Maple Group terminal. These include expansive stretches of cement and asphalt used for open yards, vehicle transport, and container storage. The UHI effect and higher surface temperatures are caused by these surfaces' increased absorption and retention of heat (Oke, 1982; Mohajerani et al., 2017). The dominance of heat-retentive structures in the port zone is further highlighted by the dark red colour of warehouses and industrial buildings. Additionally, roads are shown in black to represent their function as extra heat sources because of their high thermal conductivity and poor albedo.

The Pernis residential neighbourhood, which is surrounded by green infrastructure, contrasts sharply with the terminal's enormous, exclusively treeless area, forming a clear, visually catching spatial conflict of two different land uses. This separation supports significant variations in thermal performance and human comfort throughout the research region, which also reflects variations in land use and urban design. Because of this, the map was utilised to identify measures to mitigate heat, indicate the microclimatic hotspots in the harbour, and offer recommendations for improving thermal resistance in both the residential as well as port area.

4.2 Field Measurement

Air Temperature, Relative Humidity, Wind Speed, Globe Temperature, Heat Index and Wet Bulb Globe Temperature (WBGT) were among the field data gathered at each station. WBGT measurement has the advantage of being able to incorporate temperature, humidity, wind, and radiant heat, making it a more complete indicator of possible heat strain than air temperature alone. This is especially important in port and industrial settings where workers are subjected to complicated thermal loads from heat-retentive surfaces and solar

radiation. The open terminal (T2) and container (T3) locations continuously had higher WBGT and heat index values than the waterfront (T1), as shown by the filtered data and summary statistics. This indicates that surface materials have an impact on local heat stress.

Line graphs of mean values during the measurement period at all three sites are presented as Figures 9-13.

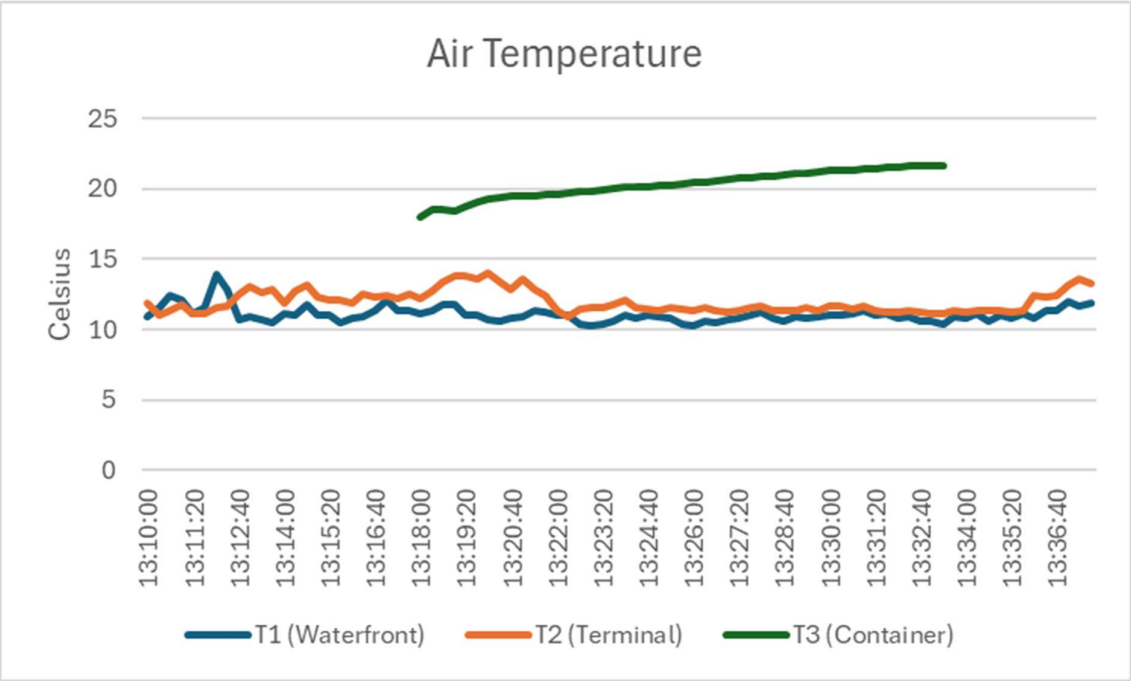

Figure 9
Time series of air temperature (°C) measured at the three pilot site locations: T1 (Waterfront), T2 (Open Container Landscape), and T3 (Confined Container) on March 31, 2025. The graph illustrates the variation in ambient air temperature across distinct microenvironments within the port terminal.

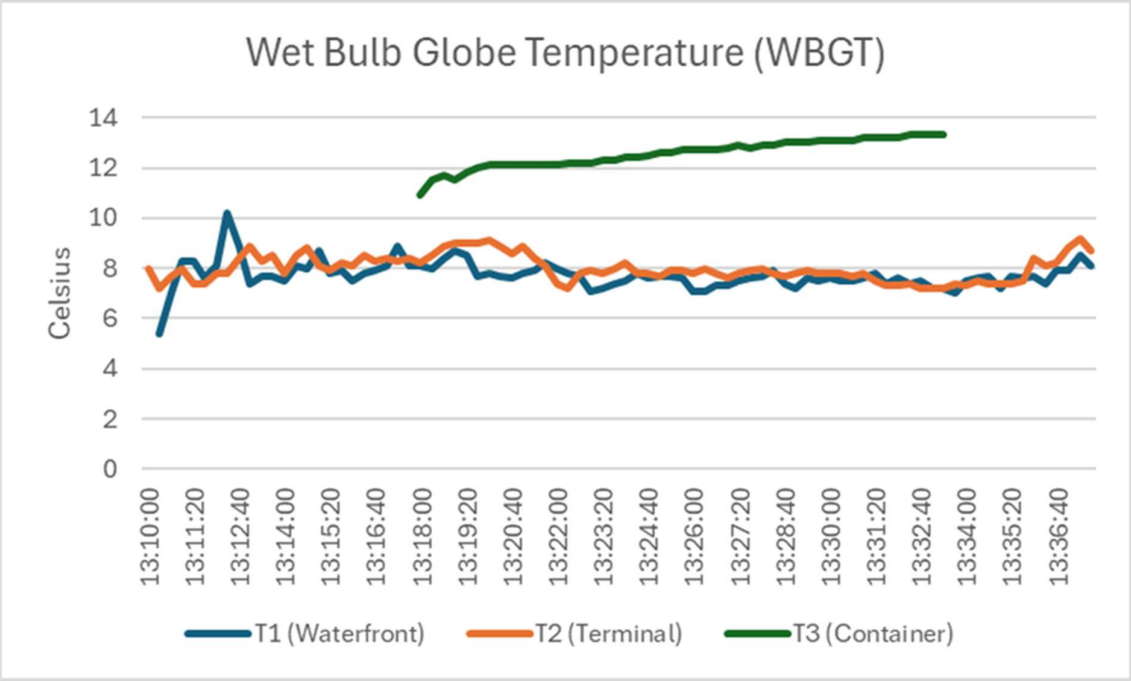

Figure 10

Wet Bulb Globe Temperature (WBGT, °C) at each measurement site, indicating the composite heat stress experienced by workers, accounting for temperature, humidity, wind speed, and radiant heat. Elevated WBGT values in T3 emphasize the risk of heat accumulation in enclosed spaces.

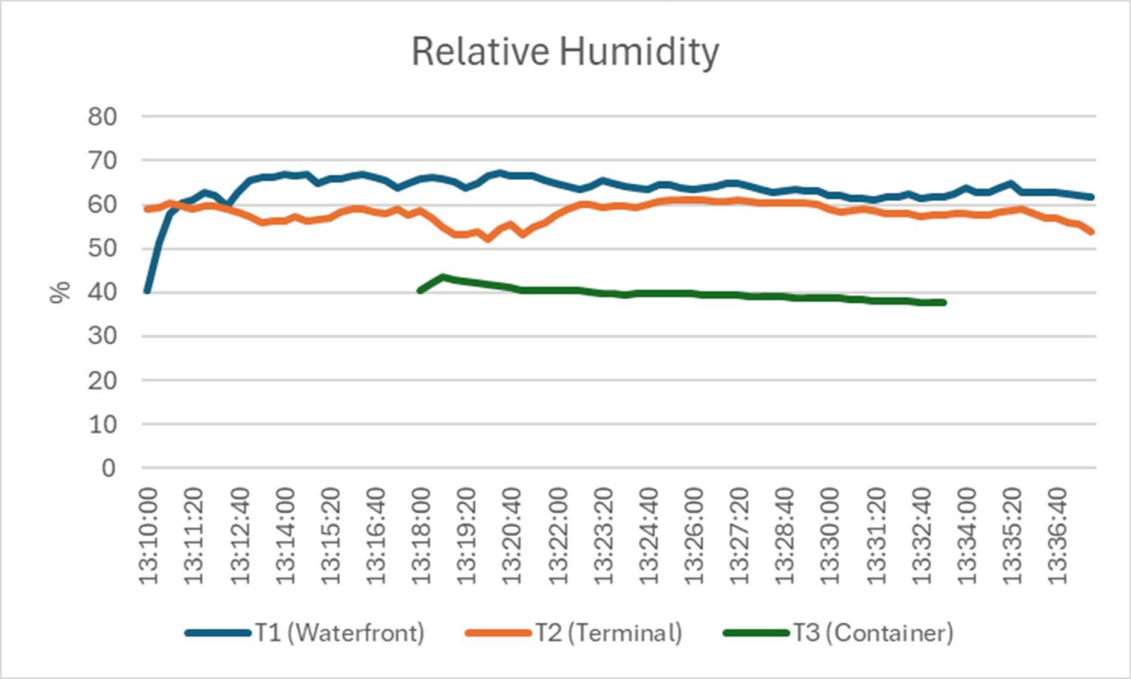

Figure 11

Relative humidity (%) trends at the three pilot site locations. The graph demonstrates the influence of enclosure and proximity to water on local moisture levels, with the highest values consistently observed at the waterfront (T1) and the lowest inside the container (T3).

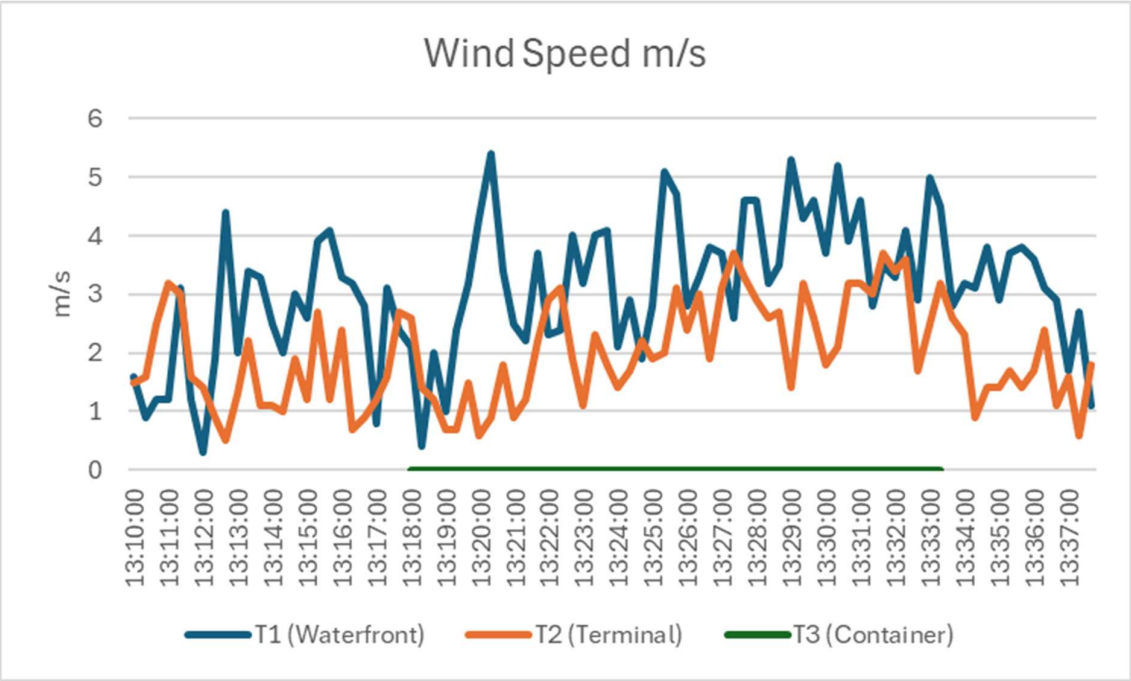

Figure 12
Wind speed (m/s) measured at T1, T2, and T3. The data reveal significant differences in ventilation, with the waterfront (T1) benefiting from higher wind speeds and the container (T3) showing zero wind speed contributing to heat retention.

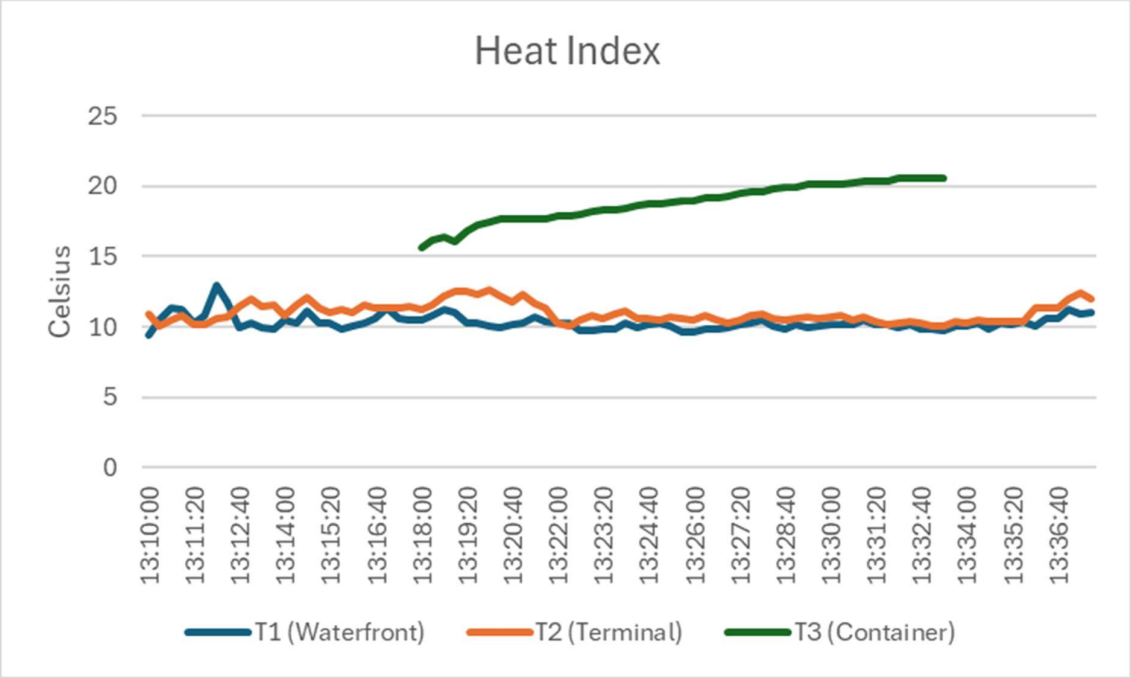

Figure 13
Heat index (°C) calculated for each measurement location, representing the perceived temperature by combining air temperature and relative humidity. The graph highlights how both temperature and humidity contribute to thermal comfort and heat stress across different port microenvironments.

4.3 Material Thermal Behaviour

The Pernis pilot site's materials-thermal behaviour link provides a powerful illustration of how materials and urban architecture directly influence microclimatic conditions in industrial port settings. The area's industrial surfaces, residential blocks, waterfront infrastructure, and urban vegetation are contrasting, each of which contributes unique microclimatic impacts and thermal signatures.

Each site's environmental data illustrates how local microclimate and material characteristics interact. With mild globe temperatures (22.05°C), T1, which is along the waterfront and next to open water and mixed surfaces, has the lowest average air temperature (11.14°C) and the highest relative humidity (63.3%). Due to its high specific heat capacity and ability to function as a buffer for heat, water helps to reduce temperature swings and increase humidity, which helps to prevent heat buildup even during periods of maximum sun exposure. The average wind speed here is 2.99 m/s, which promotes convective cooling and stabilises the microclimate even more.

T2 (Terminal), on the other hand, is in an area that is primarily paved by concrete and asphalt. This location has the greatest average globe temperature (24.08°C), the lowest relative humidity (58.7%), and a slightly higher average air temperature (11.87°C). Because of their high thermal mass and low albedo, these materials absorb and reradiate large quantities of solar energy, raising the temperature of the surface and surrounding air. Heat absorption is made worse by the lack of vegetation and shade, and convective cooling is lessened by the slower breeze (1.97 m/s) than along the riverbank. The end consequence is a microclimate that is more likely to experience UHI effects in industrial settings.

When T3 is placed inside a shipping container, the most noticeable thermal difference is seen there. relative humidity is much lower here (39.7%), and the average air temperature (20.31°C) and globe temperature (21.13°C) are much higher than at the other locations. Due

to its high thermal conductivity and low thermal inertia (capacity to withstand thermal changes), the metal structure of the container absorbs and transmits solar radiation quickly, raising the inside temperature considerably. The steadily rising temperatures can be seen in Figures 8, 9 and 12, as heat is trapped by a lack of ventilation, resulting in a microenvironment with high temperatures and little airflow. The wind speed data at T3, which continuously registers 0.0 m/s, supports this, showing stagnant air and no cooling from the wind at all. The dangerous thermal environment produced by the combination of material qualities and enclosure effects is highlighted by the much higher heat index and WBGT values at T3.

By methodically comparing microclimatic data from the three different measurement zones, the following section interprets the findings and delves into the meaning, importance, and relevance of the results of the field data.

5. Discussion

5.1 Interpretation of Findings

The Maple Group terminal's field measurements and QGIS spatial analysis show clear variation in thermal performance, impermeable surfaces continuously recording the highest temperatures during periods of maximum solar exposure. Furthermore, it is important to note that, despite the brief overlap of the tracker measurements and the relatively cold ambient conditions on the day during fieldwork, the data revealed substantial temperature differences between T3 and the other two locations. This highlights the strong influence of local materiality and spatial configuration on microclimate, even under non-extreme weather. Therefore, it is reasonable to expect that these results would be even more extreme during summer heatwaves, intensifying heat risks. Furthermore, the site's microclimatic data and visual documentation highlight how important spatial organisation and a scarcity of green infrastructure are in escalating heat stress. In industrial areas such as Pernis, the lack of

vegetation reduces the cooling effects of shading and evaporation, and large, neighbouring buildings and narrow ventilation corridors prevent heat dissipation, resulting in high temperatures that last well into the night (Bowler et al., 2010; Klok et al., 2012).

The empirical results from the Pernis pilot site have provided a better understanding of thermal variability. Thus, the results of this study could encourage adjustments to material choice and spatial arrangement to improve the performance of thermal microenvironments in industrial port regions. Strategies for climate adaptation to reduce heat stress are outlined in the following section.

5.2 Implications for Focused Recommendations

As seen in Figure 8 and its corresponding ground-level image, the open container landscape (T2) is distinguished by its paved areas and lack of shade. WBGT measurements were 13.4 ± 0.8 °C, globe temperatures peaked at 24.1 ± 1.5 °C, and average air temperatures were 11.9 ± 0.7 °C. The average wind speed in this area was 2.0 ± 0.8 m/s. High global temperatures and moderate wind indicate that heat stress in this setting is mostly caused by solar radiation, although airflow offers considerable protection. Heat accumulation occurs throughout the day because of the absence of vegetation and the domination of heat-retentive materials. The findings here highlight the necessity of solutions that target surface heat retention as well as direct sun exposure. According to research on urban greening, localised cooling can probably be achieved with even relatively minimal plants or a modular green wall. Heat buildup may be further reduced by choosing high-albedo materials for surfaces and optimising building layouts to encourage airflow (Akbari & Kolokotsa, 2016; Gartland, 2008). It has been demonstrated that these cool pavement techniques greatly lower surface temperatures, often by several degrees Celsius, which lowers the total thermal load in industrial regions (Aleksandrowicz et al., 2017). To minimise any negative effects like increased reflected heat, these pavements work best when paired with other cooling strategies

like more vegetation or thoughtful shading. The implementation of high-albedo cool pavements could be a feasible and scalable adaptation strategy. In port environments, these adaptations are crucial when combined with operational adjustments like designating areas for shaded rest and shifting demanding outdoor work to cooler times of the day.

With the greatest average wind speed across all locations (3.0 ± 1.2 m/s), T1 consistently reported the lowest air temperatures (11.1 ± 0.7 °C) and lower globe temperatures (22.0 ± 2.3 °C). T1 also had the highest relative humidity (63.3 ± 3.4 %), which is evidence of the nearby water's cooling effect. Therefore, the data support the relevance of ventilation in reducing heat stress and the cooling impact of water bodies, which means that optimising the connection between waterfronts and operating areas can be a successful passive cooling technique for industrial port architecture. To make efficient use of evaporative cooling and natural breezes, recommendations could include locating rest areas, administrative buildings, or the most heat-sensitive tasks close to the water's edge. Improving thermal comfort with temperature control could be supported by keeping orientation and air corridors exposed to the waterfront, helping improve wind penetration in the terminal's interior.

The heat profile of the enclosed container (T3), shown in Figure 7, is significantly different. In addition to globe temperatures (21.1 ± 1.6 °C) and WBGT (15.4 ± 1.0 °C), air temperatures within the container averaged 20.3 ± 1.0 °C, which was almost twice as high as those recorded in the open zones. Crucially, relative humidity was the lowest across all zones (39.7 ± 1.4 %), and wind speed was always zero. The danger of heat buildup in confined, inadequately ventilated metal structures, a prevalent characteristic of industrial ports, is best shown by this setting. Even in mild ambient circumstances, heat builds up quickly and persistently due to steel's strong thermal conductivity and the lack of ventilation. It is therefore a crucial recommendation for these areas to concentrate on improving ventilation

and lowering solar heat gain. When it comes to container exteriors, reflective coatings or shading can decrease heat absorption, while passive ventilation options like vents or roof openings can help with air exchange. Additionally, it is necessary to implement operational safety measures, such as limiting the amount of time that employees are exposed to containers during warm weather and coordinating loading and unloading during cooler hours of the day.

The data show that thermal risks are heavily site-specific. This means it is unlikely that a single solution for heat mitigation will have any substantial impact. Interventions would need to be customised to each microenvironment's unique thermal challenges instead. Shade and surface reflectivity should be prioritised for open, sun-exposed areas. For example, ventilation and safety procedures are critical for enclosed spaces and natural cooling mechanisms should be identified for areas adjacent to the waterfront, preserving and perhaps enhancing these relieving effects. Furthermore, as this study shows, making use of regular microclimatic monitoring could provide helpful data to guide long-term development plans, along with immediate responses to heat waves, for example.

Most notably, the confined container environment (T3) exhibited substantially higher air temperatures (20.3 ± 1.0°C) compared to both the open container landscape (11.9 ± 0.7°C) and waterfront (11.1 ± 0.7°C), despite relatively low relative humidity (39.7% compared to 58.7% and 63.3%, respectively). Coupled with the high WBGT values (15.4 ± 1.0°C) and the lack of wind (0.0 m/s), this temperature difference stresses how important ventilation is to prevent excessive heat in enclosed metal constructions. Passive ventilation techniques, including strategically placed vents or reflective exterior coatings that lower solar heat gain, could enhance these spaces' thermal performance.

The waterfront location (T1) consistently records the lowest temperatures despite variable wind conditions (3.0 ± 1.2 m/s), which further demonstrates the cooling effect of

proximity to water bodies. To take advantage of this natural cooling mechanism, industrial port planning may benefit from optimising the connectivity between working areas and water bodies. This could be achieved, for example, by arranging worker rest areas, or heat-sensitive operations close to waterfront spaces. Furthermore, the higher wind speeds observed along the waterfront emphasise how crucial it is to maintain and improve air corridors in industrial layouts to promote natural ventilation across the property. The open container landscape (T2) showed intermediate thermal conditions but significantly higher globe temperatures (24.1 ± 1.5°C versus 22.0 ± 2.3°C at the waterfront), suggesting significant absorption of solar radiation, and suggesting that using temporary shade structures or high-albedo surface materials in these large operating areas could be beneficial.

It should be mentioned that, as this field measurements of all three trackers overlap for a short window, it fails to measure the thermal conditions are dynamic and react to shifting environmental factors throughout the day. This temporal variability implies that operational scheduling, especially for activities carried out in enclosed containers or on exposed hardscaped surfaces, could be optimised to reduce worker exposure to periods of peak heat stress. The importance of considering multiple thermal indices when assessing heat stress risk is further highlighted by the notable differences in WBGT values between the three zones (12.6 ± 0.9°C, 13.4 ± 0.8°C and 15.4 ± 1.0°C for T1, T2, and T3, respectively). This is because different indices capture different aspects of the thermal environment.

The UHI impact will pose a growing danger to people's comfort and health in urban and industrial regions as climate change ramps up. Because of the combined effects of climate change and local industrial morphology, worker health may no longer be adequately protected by conventional coping mechanisms like rest periods and water. According to recent research, even small increases in the surrounding temperature can have a substantial impact on the risk of occupational heat stress, lower productivity, and raise the possibility of

accidents at work (Jacobs et al., 2019; Bowler et al., 2010). Understanding and reducing these thermal risks is crucial in Rotterdam Harbour, where there are high physical demands and even greater stakes for operational continuity. This is true not only to protect worker health but also to ensure the long-term resilience of the port's vital infrastructure.

Therefore, tackling the heat island effect in Rotterdam Harbour is a social and occupational health issue as well as an urban climate adaptation issue. To protect Rotterdam's harbour workers from the escalating heat, this study hopes to identify the precise morphological factors that increase heat retention and slow down cooling. This will ultimately support a safer, healthier, and more sustainable port environment.

5.3 Limitations and Future Research

It is important to further address the limitations. Firstly, field data collection was done on March 31st, and the Netherlands usually experiences the most intense UHI effects and related thermal stress during the peak summer months (Heusinkveld et al., 2010; van der Hoeven & Wandl, 2018). Therefore, the microclimatic gradients and temperature differences that have been observed could not fully reflect the seasonal effects that citizens and workers endure during heat waves. Given that the data was gathered over a very brief period is another limitation of this study. For future studies to fully capture the range of microclimatic variability, data collection covering the warmest times over a longer period should be conducted. Additionally, it was not practical to determine the precise amount of anthropogenic heat, meaning activities that raise local air and surface temperatures. This includes manufacturing, burning fuel, and operating heavy machinery, all of which produce this anthropogenic heat (Sailor, 2011). This direct measurement or calculation is primarily difficult because it requires distinguishing between solar-derived heat and anthropogenic heat emissions in such a complicated industrial setting, where the two sources overlap, and the data requirements would be too great for the scale of this study.

The fact that the study is constrained by the time coverage and resolution of the available satellite and GIS information presents another limitation. Although imagery from satellites is useful for capturing patterns of land cover on a large scale, it may not be able to detect variation in surface materials or microclimatic conditions on a smaller scale, especially in complex industrial areas. Furthermore, despite being quite extensive, the BGT dataset is updated regularly and may not properly reflect the current site-level changes in infrastructure or land use.

Future research should also focus on how microclimatic variation directly affects human health. While this study focuses on regional patterns of thermal risk, it does not measure health effects like heat stress incidence, productivity loss, or specific exposure to vulnerable populations (Pogačar et al., 2018). A more thorough analysis of the relationships between urban design, microclimate, and health outcomes might be possible by working with public health organisations like GGD Rotterdam. In industrial and port settings, where occupational exposure to severe heat is becoming a major problem due to climate change, research like this would be very valuable in creating effective responses.

As global temperatures continue to rise, they are fuelling the UHI effect, intensifying the heat in cities and making industrial zones even more formidable hotspots. Not only are the findings of this study relevant to Rotterdam, but they also provide an important direction for other port cities around the world that are navigating the challenges brought on by higher industrialisation, rapidly growing cities, and the growing effects of climate change.

7. References

Abbassi, Y., Ahmadikia, H., & Baniasadi, E. (2019). Prediction of pollution dispersion under urban heat island circulation for different atmospheric stratification. *Building and Environment, 168*, 106374. https://doi.org/10.1016/j.buildenv.2019.106374

Aflaki, A., Mirnezhad, M., Ghaffarianhoseini, A., Ghaffarianhoseini, A., Omrany, H., Wang, Z., & Akbari, H. (2017). Urban heat island mitigation strategies: A state-of-the-art review on Kuala Lumpur, Singapore and Hong Kong. *Cities, 62*, 131–145. https://doi.org/10.1016/j.cities.2016.09.003

Akbari, H., & Kolokotsa, D. (2016). Three decades of urban heat islands and mitigation technologies research. *Energy and Buildings, 133*, 834–842. https://doi.org/10.1016/j.enbuild.2016.09.067

Alavipanah, S., Schreyer, J., Haase, D., Lakes, T., & Qureshi, S. (2018). The effect of multi-dimensional indicators on urban thermal conditions. *Journal of Cleaner Production, 177*, 115–123. https://doi.org/10.1016/j.jclepro.2017.12.187

Aleksandrowicz, O., Vuckovic, M., Kiesel, K., & Mahdavi, A. (2017). Current trends in urban heat island mitigation research: Observations based on a comprehensive research repository. *Urban Climate, 21*, 1–26. https://doi.org/10.1016/j.uclim.2017.04.002

Arifwidodo, S. D. (2015). Factors contributing to urban heat island in Bangkok, Thailand. *ARPN Journal of Engineering and Applied Sciences, 10*(15), 6435–6439.

Armson, D., Stringer, P., & Ennos, A. (2012). The effect of tree shade and grass on surface and globe temperatures in an urban area. *Urban Forestry & Urban Greening*, 11(3), 245–255. https://doi.org/10.1016/j.ufug.2012.05.002

Azevedo, J. A., Chapman, L., & Muller, C. L. (2016). Quantifying the daytime and night-time urban heat island in Birmingham, UK: A comparison of satellite-derived land surface temperature and high-resolution air temperature observations. *Remote Sensing, 8*(2), 153. https://doi.org/10.3390/rs8020153

Brode, P., Fiala, D., Blazejczyk, K., Holmér, I., Jendritzky, G., Kampmann, B., Tinz, B., & Havenith, G. (2012). Deriving the operational procedure for the universal thermal climate index (UTCI). *International Journal of Biometeorology, 56*(3), 481–494. https://doi.org/10.1007/s00484-011-0454-1

Burian, S. J., Brown, M. J., & Linger, S. P. (2002). Morphological analyses using 3D building databases: Los Angeles, California (Report LA-UR-02-0781). *Los Alamos National Laboratory*.

Chen, A., Zhao, X., Yao, L., & Chen, L. (2016). Application of a new integrated landscape index to predict potential urban heat islands. *Ecological Indicators, 69*, 828–835. https://doi.org/10.1016/j.ecolind.2016.05.045

Chen, X., Wang, Y., & Li, Z. (2019). Anthropogenic heat flux and land surface temperature in industrial parks: A case study of Shanghai. *Environmental Research Letters, 14*(8), 084012.

Chen, Y., Wang, Y., & Zhou, D. (2021). Knowledge map of urban morphology and thermal comfort: A bibliometric analysis based on CiteSpace. *Buildings, 11*(10), 427. https://doi.org/10.3390/buildings11100427

Clark, V. L. P. (2016). Mixed methods research. *The Journal of Positive Psychology, 12*(3), 305–306. https://doi.org/10.1080/17439760.2016.1262619

Cui, Y., Yan, D., Hong, T., & Ma, J. (2017). Temporal and spatial characteristics of the urban heat island in Beijing and the impact on building design and energy performance. *Energy, 130*, 286–297. https://doi.org/10.1016/j.energy.2017.04.053

Deilami, K., Kamruzzaman, M., & Liu, Y. (2018). Urban heat island effect: A systematic review of spatio-temporal factors, data, methods, and mitigation measures. *International Journal of Applied Earth Observation and Geoinformation, 67*, 30–42. https://doi.org/10.1016/j.jag.2017.12.009

Derdouri, A., Wang, R., Murayama, Y., & Osaragi, T. (2020). Understanding the links between LULC changes and SUHI in cities: Insights from two-decadal studies (2001–2020). *Remote Sensing, 13*(18), 3654. https://doi.org/10.3390/rs13183654

DiNapoli, C., Messeri, A., Novák, M., Rio, J., Wieczorek, J., Morabito, M., Silva, P., Crisci, A., & Pappenberger, F. (2021). The universal thermal climate index as an operational forecasting tool of human biometeorological conditions in Europe. In E. L. Kruger (Ed.), *Applications of the universal thermal climate index UTCI in biometeorology: Latest developments and case studies* (pp. 193–208). Springer.

European Centre for Environment and Health. (2016). *Heatwaves and health: Guidance on warning-system development.* World Health Organization.

European Centre for Environment and Health. (2016). *Urban green space interventions and health: A review of impacts and effectiveness.* WHO Regional Office for Europe. Retrieved from WHO.

Fonseca, F., Paschoalino, M., & Silva, L. (2022). Health and well-being benefits of outdoor and indoor vertical greening systems: A review. *Sustainability, 15*(5), 4107. https://doi.org/10.3390/su15054107

Gartland, L. M. (2012). *Heat Islands.* Routledge eBooks. https://doi.org/10.4324/9781849771559

Giles-Corti, B., Lowe, M., & Arundel, J. (2020). Achieving the SDGs: Evaluating indicators to be used to benchmark and monitor progress towards creating healthy and sustainable cities. *Health Policy, 124*(6), 581–590. https://doi.org/10.1016/j.healthpol.2019.03.001

Kleerekoper, L. (2016). *Urban climate design: Improving thermal comfort in Dutch neighbourhoods* [Dissertation, Delft University of Technology]. A+BE | Architecture and the Built Environment. https://doi.org/10.7480/abe.2016.11

Giorgio, G. A., Ragosta, M., & Telesca, V. (2017). Climate variability and industrial-suburban heat environment in a Mediterranean area. *Sustainability, 9*(5), 775. https://doi.org/10.3390/su9050775

Gober, P., Brazel, A., Quay, R., Myint, S., Grossman-Clarke, S., Miller, A., & Rossi, S. (2009). Using watered landscapes to manipulate urban heat island effects: How much water will it take to cool Phoenix? *Journal of the American Planning Association, 76*(1), 109–121. https://doi.org/10.1080/01944360903433113

Gong, P., Li, X., Wang, J., Bai, Y., Chen, B., Hu, T., Liu, X., Xu, B., Yang, J., Zhang, W., & Zhou, Y. (2019). Annual maps of global artificial impervious area (GAIA) between 1985 and 2018. *Remote Sensing of Environment, 236*, 111510. https://doi.org/10.1016/j.rse.2019.111510

Güller, C., & Toy, S. (2023). The impacts of urban morphology on urban heat islands in housing areas: The case of Erzurum, Turkey. *Sustainability, 16*(2), 791. https://doi.org/10.3390/su16020791

Harmay, N. S. M., & Choi, M. (2023). The urban heat island and thermal heat stress correlate with climate dynamics and energy budget variations in multiple urban environments. *Sustainable Cities and Society, 91*, 104422. https://doi.org/10.1016/j.scs.2023.104422

Heusinkveld, B. G., Steeneveld, G. J., van Hove, L. W. A., Jacobs, C. M. J., & Holtslag, A. A. M. (2010). Spatial variability of the Rotterdam urban heat island as influenced by urban land use. *Journal of Geophysical Research: Atmospheres, 115*(D2), D02108. https://doi.org/10.1029/2009JD012374

Howard, L. (1833). *The climate of London: Deduced from meteorological observations made in the metropolis and at various places around it* (Vol. 3). Harvey and Darton, J. and A. Arch, Longman, Hatchard, S. Highley [and] R. Hunter.

Hsu, A., Sheriff, G., Chakraborty, T., & Manya, D. (2021). Disproportionate exposure to urban heat island intensity across major US cities. *Nature Communications, 12*. https://doi.org/10.1038/s41467-021-22799-5

Hu, Y., Dai, Z., & Guldmann, J. (2020). Modeling the impact of 2D/3D urban indicators on the urban heat island over different seasons: A boosted regression tree approach. *Journal of Environmental Management, 266*, 110424. https://doi.org/10.1016/j.jenvman.2020.110424

Huang, J., Kong, F., Yin, H., Middel, A., Liu, H., & Meadows, M. E. (2023). Green roof effects on urban building surface processes and energy budgets. *Energy Conversion and Management, 287*, 117100. https://doi.org/10.1016/j.enconman.2023.117100

Huang, Q., & Lu, Y. (2018). Urban heat island research from 1991 to 2015: A bibliometric analysis. *Theoretical and Applied Climatology, 131*(3–4), 1055–1067. https://doi.org/10.1007/s00704-016-2025-1

IPCC. (2014). *Impacts, adaptation, and vulnerability. Part A: Global and sectoral aspects. Contribution of Working Group II to the Fifth Assessment Report of the Intergovernmental Panel on Climate Change.* Cambridge University Press.

Jacobs, C., Singh, T., Gorti, G., Iftikhar, U., Saeed, S., Syed, A., Abbas, F., Ahmad, B., Bhadwal, S., & Siderius, C. (2019). Patterns of outdoor exposure to heat in three South Asian cities. *Science of the Total Environment, 674*, 264–278. https://doi.org/10.1016/j.scitotenv.2019.04.087

Jiang, Y., Hou, L., Shi, T., & Ning, Y. (2018). Spatial zoning strategy of urbanization based on urban climate co-movement: A case study in Shanghai mainland area. *Sustainability, 10*(8), 2706. https://doi.org/10.3390/su10082706

Jiang, S., Zhou, W., Li, W., Qian, Y., Zhao, J., & Lu, Y. (2021). How do urban morphological factors influence land surface temperature? A case study of Nanjing, China. *Sustainable Cities and Society, 69*, 102846. https://doi.org/10.1016/J.SCS.2021.102846

Kappou, S., Souliotis, M., Papaefthimiou, S., Panaras, G., Paravantis, J. A., Michalena, E., Hills, J. M., Vouros, A. P., Ntymenou, A., & Mihalakakou, G. (2022). Cool pavements: State of the art and new technologies. In V. Costanzo (Ed.), *Sustainability, 14*, 5159. https://doi.org/10.3390/su14095159

Klok, L., Zwart, S., Verhagen, H., & Mauri, E. (2012). The surface heat island of Rotterdam and its relationship with urban surface characteristics. *Resources Conservation and Recycling, 64*, 23–29. https://doi.org/10.1016/j.resconrec.2012.01.009

Klok, L., Ten Broeke, H., Van Harmelen, T., Verhagen, H., Kok, H., TNO Bouw en Ondergrond, & Waterwatch BV. (2010, July). *Ruimtelijke verdeling en mogelijke oorzaken van het hitte-eiland effect* (TNO-034-UT-2010-01229_RPT-ML). TNO-rapport (pp. 3–78). https://publications.tno.nl/publication/102468/uV8TLr/UT-2010-01299.pdf

Kumar, P., Zavala-Reyes, J. C., Tomson, M., & Kalaiarasan, G. (2022). Understanding the effects of roadside hedges on the horizontal and vertical distributions of air pollutants in street canyons. *Environment International, 158*, 106883. https://doi.org/10.1016/j.envint.2021.106883

Lin, P., Lau, S. S. Y., Qin, H., & Gou, Z. (2017). Effects of urban planning indicators on urban heat island: A case study of pocket parks in high-rise high-density environment. *Landscape and Urban Planning, 168*, 48–60. https://doi.org/10.1016/j.landurbplan.2017.09.024

Liu, S., Zhang, J., Li, J., Li, Y., Zhang, J., & Wu, X. (2021). Simulating and mitigating extreme urban heat island effects in a factory area based on machine learning. *Building and Environment, 202*, 108051. https://doi.org/10.1016/j.buildenv.2021.108051

Lopes, H. S., Vidal, D. G., Cherif, N., Silva, L., & Remoaldo, P. C. (2025). Green infrastructure and its influence on urban heat island, heat risk, and air pollution: A case study of Porto (Portugal). *Journal of Environmental Management, 376*, 124446.

Meng, Q., Hu, D., Zhang, Y., Chen, X., Zhang, L., & Wang, Z. (2021). Do industrial parks generate intra-heat island effects in cities? New evidence, quantitative methods, and contributing

factors from a spatiotemporal analysis of top steel plants in China. *Environmental Pollution, 292*, 118383. https://doi.org/10.1016/j.envpol.2021.118383

Milojevic-Dupont, S., Stewart, I. D., Dawson, R. J., poza, K. V., Kaack, L. H., Pichler, P. P., & Creutzig, F. (2023). EUBUCCO v0.1: European building stock characteristics in a common and open database for 200+ million individual buildings. *Scientific Data, 10*(1), 1–17. https://doi.org/10.1038/s41597-023-02040-2

Mirzaei, P. A. (2015). Recent challenges in modeling of urban heat island. *Sustainable Cities and Society, 19*, 200–206. https://doi.org/10.1016/j.scs.2015.04.001

Mo, Y., Xu, Y., Chen, H., & Zhu, S. (2021). A review of reconstructing remotely sensed land surface temperature under cloudy conditions. *Remote Sensing, 13*(14), 2838. https://doi.org/10.3390/RS13142838

Mohajerani, A., Bakaric, J., & Jeffrey-Bailey, T. (2017). The urban heat island effect, its causes, and mitigation, with reference to the thermal properties of asphalt concrete. *Journal of Environmental Management, 197*, 522–538. https://doi.org/10.1016/j.jenvman.2017.03.095

Mudu, P., Uscila, V., Barrdahl, M., Kulinkina, A., Staatsen, B., Swart, W., Kruize, H., Zurlyte, I., & Egorov, A. I. (2016). Development of an urban green space indicator and the public health rationale. Scandinavian Journal of Public Health. https://doi.org/10.1177/1403494815615444

Norton, B. A., Coutts, A. M., Livesley, S. J., Harris, R. J., & Williams, N. S. G. (2015). Planning for cooler cities: A framework to prioritize green infrastructure to mitigate urban heat. *Landscape and Urban Planning, 134*, 127–138. https://doi.org/10.1016/j.landurbplan.2014.10.018

Oke, T. R. (1982). The energetic basis of the urban heat island. *Quarterly Journal of the Royal Meteorological Society, 108*(455), 1–24. https://doi.org/10.1002/qj.49710845502

Oke, T. R. (1995). The heat island of the urban boundary layer: Characteristics, causes and effects. In *The urban climate* (pp. 81–107). Cambridge University Press.

Onishi, A., Cao, X., Ito, T., Shi, F., & Imura, H. (2010). Evaluating the potential for urban heat-island mitigation by greening parking lots. *Urban Forestry & Urban Greening, 9*(4), 323–332. https://doi.org/10.1016/j.ufug.2010.06.002

Ouchra, H., & Belangour, A. (2021). Object detection approaches in images: A survey. *Proceedings of SPIE, 11878*, 132–141. https://doi.org/10.1117/12.2601452

Page, M. J., McKenzie, J. E., Bossuyt, P. M., Boutron, I., Hoffmann, T. C., Mulrow, C. D., Shamseer, L., Tetzlaff, J. M., Akl, E. A., Brennan, S. E., Chou, R., Glanville, J., Grimshaw, J. M., Hróbjartsson, A., Lalu, M. M., Li, T., Loder, E. W., Mayo-Wilson, E., McDonald, S., . . . Moher, D. (2021). The PRISMA 2020 statement: an updated guideline for reporting systematic reviews. BMJ, n71. https://doi.org/10.1136/bmj.n71

Parker, J. (2021). The Leeds urban heat island and its implications for energy use and thermal comfort. *Energy & Buildings, 235*, 110636. https://doi.org/10.1016/j.enbuild.2020.110636

Parker, J. (2024). Characteristics of air temperature and thermal comfort in the grey and green spaces of an urban heat island. *Sustainable Environment, 10*(1).

Peng, J., Dan, Y., Qiao, R., Liu, Y., Dong, J., & Wu, J. (2020). How to quantify the cooling effect of urban parks? Linking maximum and accumulation perspectives. Remote Sensing of Environment, 252, 112135. https://doi.org/10.1016/j.rse.2020.112135

Peng, Z., Jia, L., Li, L., Quan, S. J., & Yang, P. P.-J. (2017). How the roofing morphology and housing form affect energy performance of Shanghai's workers' village in urban regeneration. Energy Procedia, 142, 3075-3082.

Pogačar, T., Casanueva, A., & Kozjek, K. (2018). The effect of hot days on occupational heat stress in the manufacturing industry: Implications for workers' well-being and productivity. *International Journal of Biometeorology, 62*(7), 1251–1264. https://doi.org/10.1007/s00484-018-1530-6

Richards, K., & Oke, T. R. (2002). Validation and results of a scale model of dew deposition in urban environments. International Journal of Climatology, 22(15), 1915-1933. https://doi.org/10.1002/joc.856

Roesler, J., Sen, S., & University of Illinois at Urbana-Champaign. (2016). *Impact of pavements on the urban heat island* (Center for Highway Pavement Preservation & US Department of Transportation–Research and Innovative Technology Administration). https://www.chpp.egr.msu.edu/wp-content/uploads/2014/04/CHPP-Report-UIUC2B-2016.pdf

Sailor, D. J. (2011). A review of methods for estimating anthropogenic heat and moisture emissions in the urban environment. International Journal of Climatology, 31(2), 189-199. https://doi.org/10.1002/joc.2106

Santamouris, M., Cartalis, C., Synnefa, A., & Kolokotsa, D. (2015). On the impact of urban heat island and global warming on the power demand and electricity consumption of buildings—A review. Energy and Buildings, 98, 119-124. https://doi.org/10.1016/j.enbuild.2014.09.052

Taylor, J., Wilkinson, P., Picetti, R., Symonds, P., Heaviside, C., Macintyre, H. L., Davies, M., Mavrogianni, A., & Hutchinson, E. (2017). Comparison of built environment adaptations to heat exposure and mortality during hot weather, West Midlands region, UK. *Environment International, 111*, 287–294. https://doi.org/10.1016/j.envint.2017.11.005

Tokaya, J., Kranenburg, R., Timmermans, R., Coenen, P., Kelly, B., Hullegie, J., Megaritis, T., & Valastro, G. (2024). The impact of shipping on the air quality in European port cities with a detailed analysis for Rotterdam. *Atmospheric Environment X, 23*, 100278. https://doi.org/10.1016/j.aeaoa.2024.100278

Tzoulas, K., Korpela, K., Venn, S., Yli-Pelkonen, V., Kaźmierczak, A., Niemela, J., & James, P. (2007). Promoting ecosystem and human health in urban areas using green infrastructure: A

literature review. *Landscape and Urban Planning, 81*(3), 167–178. https://doi.org/10.1016/j.landurbplan.2007.02.001

Van Der Hoeven, F., & Wandl, A. (2018). Hotterdam: Mapping the social, morphological, and land-use dimensions of the Rotterdam urban heat island. *Urbani Izziv, 29*(1), 58–72. https://doi.org/10.5379/urbani-izziv-en-2018-29-01-001

Van Hove, L., Jacobs, C., Heusinkveld, B., Elbers, J., Van Driel, B., & Holtslag, A. (2014). Temporal and spatial variability of urban heat island and thermal comfort within the Rotterdam agglomeration. *Building and Environment*, *83*, 91-103. https://doi.org/10.1016/j.buildenv.2014.08.029

Voogt, J., & Oke, T. (2003). Thermal remote sensing of urban climates. *Remote Sensing of Environment*, *86*(3), 370-384. https://doi.org/10.1016/S0034-4257(03)00079-8

Weng, Q. (2009). Thermal infrared remote sensing for urban climate and environmental studies: Methods, applications, and trends. *ISPRS Journal of Photogrammetry and Remote Sensing, 64*(4), 335–344. https://doi.org/10.1016/j.isprsjprs.2009.03.007

Wong, M. S., & Nichol, J. E. (2012). Spatial variability of frontal area index and its relationship with urban heat island intensity. *International Journal of Remote Sensing, 34*(3), 885–896. https://doi.org/10.1080/01431161.2012.714509

Xia, H., Chen, Y., & Quan, J. (2018). A simple method based on the thermal anomaly index to detect industrial heat sources. *International Journal of Applied Earth Observation and Geoinformation, 73*, 627–637. https://doi.org/10.1016/j.jag.2018.08.003

Xiao, R., Weng, Q., Ouyang, Z., Li, W., Schienke, E. W., & Zhang, Z. (2008). Land surface temperature variation and major factors in Beijing, China. *Photogrammetric Engineering & Remote Sensing, 74*(4), 451–461. https://doi.org/10.14358/pers.74.4.451

Yuan, C., & Chen, L. (2011). Mitigating urban heat island effects in high-density cities based on sky view factor and urban morphological understanding: A study of Hong Kong. *Architectural Science Review, 54*(4), 305–315. https://doi.org/10.1080/00038628.2011.613644

Zhang, P., Imhoff, M. L., Wolfe, R. E., & Bounoua, L. (2010). Characterizing urban heat islands of global settlements using MODIS and nighttime lights products. *Canadian Journal of Remote Sensing, 36*(3), 185–196. https://doi.org/10.5589/m10-039

Zhang, Q., Zhou, D., Xu, D., & Rogora, A. (2022). Correlation between cooling effect of green space and surrounding urban spatial form: Evidence from 36 urban green spaces. *Building & Environment, 222*, 109375. https://doi.org/10.1016/j.buildenv.2022.109375

Zhou, D., Zhao, S., Liu, S., Zhang, L., & Zhu, C. (2014). Surface urban heat island in China's 32 major cities: Spatial patterns and drivers. *Remote Sensing of Environment, 152*, 51–61. https://doi.org/10.1016/j.rse.2014.05.017

Zhu, Z., Shen, Y., Fu, W., Zheng, D., Huang, P., Li, J., Lan, Y., Chen, Z., Liu, Q., Xu, X., & Yao, X. (2023). How does 2D and 3D of urban morphology affect the seasonal land surface temperature in Island City? A block-scale perspective. *Ecological Indicators, 150*, 110221.

8. Appendices

Appendix A: Microclimate Data by Location (13:00–13:30)

Zone	***Air Temp (°C)***	***Globe Temp (°C)***	***WBGT (°C)***	***Rel. Humidity (%)***	***Wind Speed (m/s)***
Waterfront (T1)	*11.1 ± 0.7*	*22.0 ± 2.3*	*12.6 ± 0.9*	*63.3 ± 3.4*	*3.0 ± 1.2*
Terminal (T2)	*11.9 ± 0.7*	*24.1 ± 1.5*	*13.4 ± 0.8*	*58.7 ± 2.1*	*2.0 ± 0.8*
Container (T3)	*20.3 ± 1.0*	*21.1 ± 1.6*	*15.4 ± 1.0*	*39.7 ± 1.4*	*0.0*

Appendix B. Visual Map Photo Locations Marked

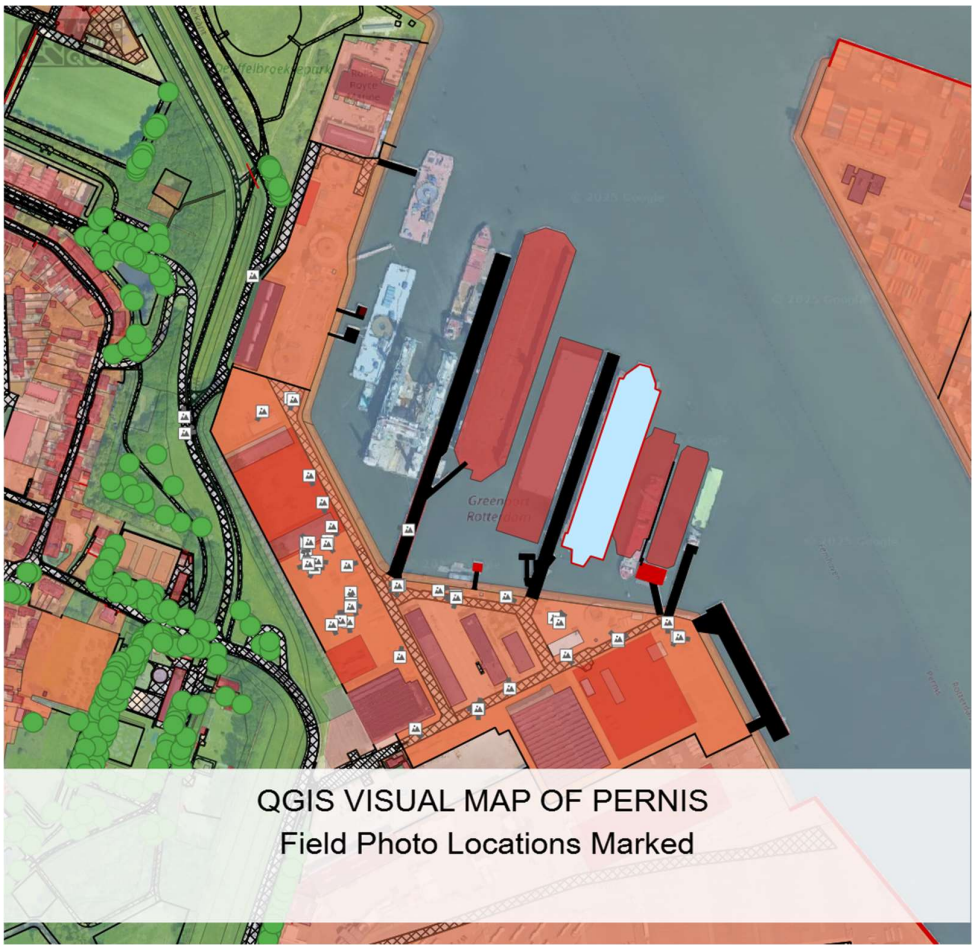

Appendix C. Fieldwork Photo Download Link

Photos Maple Group 20-03-2025

Appendix D. Download Links for QGIS and the PDOK BGT Downloader

- QGIS: https://qgis.org/download/
- PDOK BGT Downloader: https://app.pdok.nl/lv/bgt/download-viewer/